Metal vapour transport in tungsten–inert-gas welding

J. Xiang[1], F. F. Chen[1], H. Park[2,3] and A. B. Murphy[3]

[1]*CSIRO Manufacturing, PO Box 10, Clayton South VIC 3169, Australia*
[2] *Korea Institute of Materials Science, 797, Changwon-daero, Seongsan-gu, Changwon-si, Gyeongsangnam-do 51508, Republic of Korea*
[3]*CSIRO Manufacturing, PO Box 218, Lindfield NSW 2070, Australia*

Abstract: A computational model of tungsten–inert-gas (TIG) welding in argon that includes the influence of iron and chromium vapour is presented. It is found that the metal vapours are transported, mainly by convection, from the weld pool to the cathode region. Diffusion driven by temperature gradients is responsible for the metal vapours moving into the recirculating flow. This mechanism differs from that found in TIG welding in helium. Photographic evidence supports the predicted presence of metal vapour near the cathode.

Keywords: TIG welding, arc welding, gas tungsten arc welding, metal vapour, diffusion

1. Introduction

Tungsten–inert gas (TIG) welding, also known as gas tungsten arc welding, is widely used in industry to join metals, particularly stainless steels. In TIG welding, an arc in an inert gas, usually argon, helium or an argon–helium mixture, is struck between two electrodes. The upper electrode is a tungsten cathode, while the lower electrode, known as the workpiece, is the metal being welded. The arc partially melts the workpiece to form a weld pool.

It is well known that metal vapour is produced by vaporization of the weld pool surface. Until recently, it has been understood that the metal vapour is swept radially outwards by the strong convective flow in the arc and so remains close to the workpiece surface [1]. The flow is driven by the strong magnetic pinch force near the cathode tip. It is directed downwards from the cathode to the workpiece and then radially outwards near the workpiece.

However, measurements for a helium TIG arc with a stainless steel workpiece showed that metal vapour is present in the arc column and is deposited on the tungsten cathode [2]. These results were recently explained by Park et al. [3, 4], who showed that cataphoresis (diffusion driven by an electric field) led to upward diffusion of metal vapour from the weld pool towards the cathode. Previous models had used simplified treatments of diffusion and had neglected cataphoresis, and as a consequence had not predicted the upward transport of metal vapour.

Park et al. pointed out that cataphoresis will be much weaker in an argon arc than in a helium arc [4]. Measurements have generally found little or no evidence of metal vapour in the arc column or near the cathode in argon TIG welding [5]. Nevertheless, since previous models of TIG welding in argon have used strongly simplified treatments of diffusion and neglected cataphoresis, it is important to re-examine the metal vapour transport in argon TIG welding.

In this paper, we present results of a computational model of argon TIG welding that includes a full treatment of diffusion of the iron and chromium vapour produced from a stainless steel workpiece. We compare the results to those for helium TIG welding, and discuss the results in terms of the different diffusion driving forces.

2. Computational model

The computational model of TIG welding uses the methods given by Park et al. [4]. Equations for conservation of mass, momentum, energy and charge, and Ohm's law, are solved in two dimensions in the arc and electrodes, assuming local thermodynamic equilibrium. The transport of iron and chromium vapour is taken into account by solving conservation equations for the mass fraction of each metal vapour:

$$\begin{aligned} \nabla\cdot\left(\rho\boldsymbol{v}\overline{Y_{\mathrm{Fe}}}\right) &= -\nabla\cdot\overline{\boldsymbol{J}_{\mathrm{Fe}}} + S_{\mathrm{Fe}}, \\ \nabla\cdot\left(\rho\boldsymbol{v}\overline{Y_{\mathrm{Cr}}}\right) &= -\nabla\cdot\overline{\boldsymbol{J}_{\mathrm{Cr}}} + S_{\mathrm{Cr}}, \end{aligned} \qquad (1)$$

where ρ is the mass density, $\boldsymbol{v}$ is the plasma velocity, $\overline{Y_I}$ is the mass fraction of metal vapour I, $S_I = J_{\mathrm{vap}\,I}/A$ is the source term related to the rate of vaporization $J_{\mathrm{vap}\,I}$ of metal vapour I, calculated using the Hertz–Knudsen–Langmuir equation [6], and A is the cross-sectional area of the computational cell parallel to the metal surface. The mass flux of iron and chromium vapour in the case of argon TIG welding is given by

$$\begin{aligned} \overline{\boldsymbol{J}_{\mathrm{Fe}}} &= \frac{n^2}{\rho}\overline{m_{\mathrm{Fe}}m_{\mathrm{Cr}}m_{\mathrm{Ar}}}\left[\left(\overline{D^x_{\mathrm{Fe\,Cr}}}\nabla\overline{x_{\mathrm{Cr}}} + \overline{D^x_{\mathrm{Fe\,Ar}}}\nabla\overline{x_{\mathrm{Ar}}}\right) + \overline{D^E_{\mathrm{Fe}}}\,\boldsymbol{E}\right] \\ &\quad - \overline{D^T_{\mathrm{Fe}}}\nabla\ln T, \\ \overline{\boldsymbol{J}_{\mathrm{Cr}}} &= \frac{n^2}{\rho}\overline{m_{\mathrm{Fe}}m_{\mathrm{Cr}}m_{\mathrm{Ar}}}\left[\left(\overline{D^x_{\mathrm{Cr\,Fe}}}\nabla\overline{x_{\mathrm{Fe}}} + \overline{D^x_{\mathrm{Cr\,Ar}}}\nabla\overline{x_{\mathrm{Ar}}}\right) + \overline{D^E_{\mathrm{Cr}}}\,\boldsymbol{E}\right] \\ &\quad - \overline{D^T_{\mathrm{Cr}}}\nabla\ln T, \end{aligned} \qquad (2)$$

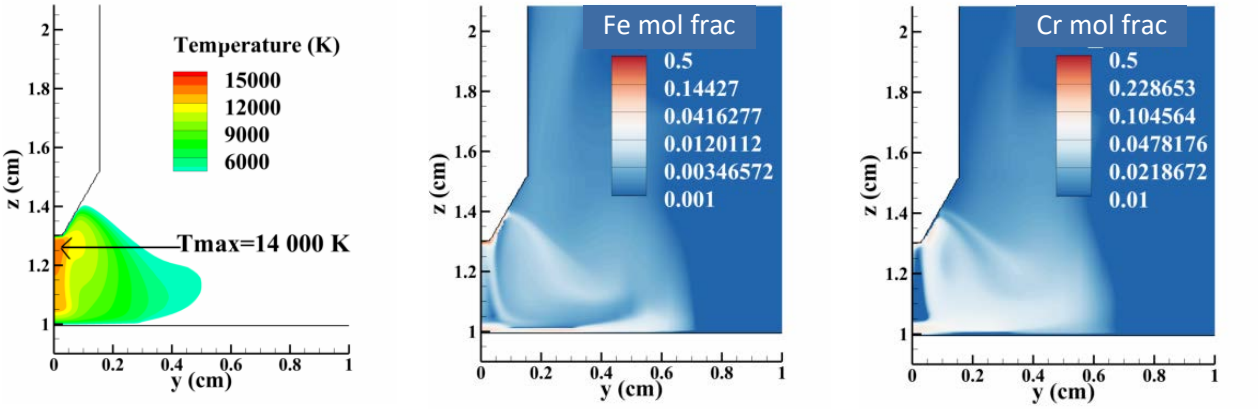

(a) (b) (c)

Fig. 1. Distributions of (a) temperature, (b) iron vapour mole fraction, (c) chromium vapour mole fraction in argon TIG welding of stainless steel.

where $\overline{m_I}$ is the average mass of the heavy species of gas I, $\overline{x_I}$ is the sum of the mole fractions of the species making up gas I, and $\overline{D_{IJ}^x}$, $\overline{D_I^E}$ and $\overline{D_I^T}$ are respectively the combined ordinary, electric field and temperature diffusion coefficients. The diffusion coefficients are calculated using the methods presented by Zhang et al [7].

3. Argon TIG welding

We present results for a 3 mm arc and an arc current of 150 A. The stainless steel is assumed to contain 79 mol% Fe and 21 mol% Cr; the other elements are neglected.

Fig. 1 shows results for an argon arc. There are significant mole fractions of iron and chromium vapours present close to the workpiece, with maximum values of 0.05 and 0.08 respectively above the weld pool. The highest concentrations occur near the cathode tip, with the iron and chromium mole fractions reaching their respective maximum values of 0.23 and 0.12 here. Large concentrations of metal vapour also occur between the electrodes, except in the central high temperature region of the arc column.

The formation of a significant concentration of metal vapour near the workpiece is consistent with the results of other modelling work [1]. However, no previous models of argon TIG welding have predicted the presence of metal vapour near the cathode. It is therefore important to examine the reasons for the transport of metal vapour to this region.

All previous models of TIG welding used approximate treatments of diffusion. These treatments only took ordinary diffusion into account, and only in an approximate manner. Further, only one metal vapour has been considered. The combined diffusion treatment used here takes into account all important driving forces, including electrical fields and temperature gradients as well as mole fraction gradients, and allows consideration of two metal vapours. The combined diffusion coefficient method is equivalent to a full multicomponent treatment, and so is much more accurate than previously used methods.

We can examine the influence of the different diffusion driving forces by setting the relevant terms to zero in Eq. (2). Fig. 2 shows the results obtained by setting $\overline{D_{\mathrm{Fe}}^E} = \overline{D_{\mathrm{Cr}}^E} = 0$ (i.e. neglecting diffusion driven by the electric field) and by setting $\overline{D_{\mathrm{Fe}}^T} = \overline{D_{\mathrm{Cr}}^T} = 0$ (i.e. neglecting diffusion driven by temperature gradients). In the former case (Fig. 2(a)), there is very little change, with the maximum mole fraction of chromium vapour near the cathode tip remaining at 0.12. In the latter case (Fig. 2(b)), the chromium mole fraction near the cathode tip is reduced to a negligible value of 0.001.The chromium mole fractions near the workpiece are unchanged in both cases. Similar results are obtained for iron vapour.

The results demonstrate that the temperature gradient terms in Eq. (2) play a critical role in the transport of metal vapour to the cathode region, while the electric field terms do not have a significant influence. Fig. 3 shows the combined temperature and electric field diffusion

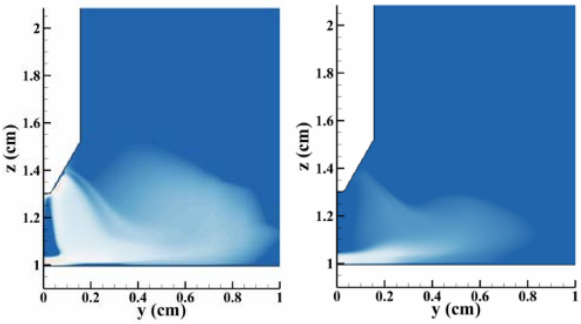

(a) (b)

Fig. 2. Distributions of chromium vapour mole fraction neglecting (a) diffusion driven by electric fields and (b) diffusion driven by temperature gradients. The mole fraction scale is the same as in Fig. 1(c).

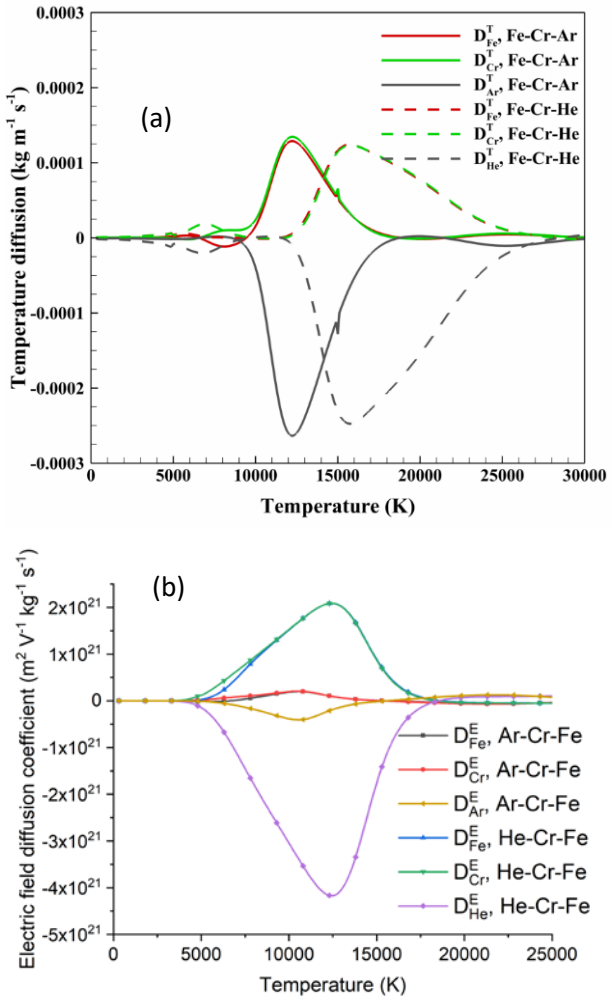

Fig. 3. Combined (a) temperature and (b) electric field diffusion coefficients for mixtures of 10% wt% iron and 10 wt% chromium with argon or helium.

coefficients for an Fe-Cr-Ar mixture. The values of $\overline{D^T_{Fe}}$ and $\overline{D^T_{Cr}}$ are negative at lower temperatures (below 10 000 K for Fe and 7000 K for Cr). Diffusion driven by temperature gradients is therefore directed towards higher temperatures in the arc fringes close to the workpiece, causing the metal vapours to diffuse upward into the recirculating flow region. The metal vapours are then convected upward and inward towards the cathode. The values of $\overline{D^T_{Fe}}$, $\overline{D^T_{Cr}}$, $\overline{D^E_{Fe}}$ and $\overline{D^E_{Cr}}$ are all strongly positive between 10 000 and 16 000 K, so the temperature and electric field diffusion are upward towards the cathode near the arc axis. This opposes the downwards convective flow, tending to confine the metal vapour near the cathode tip and leading to the 'hollow' metal vapour distribution apparent in Fig. 1.

4. Helium TIG welding

The metal vapour distributions for helium, shown in Fig. 4, differ markedly from those predicted for argon. In particular, both chromium and iron vapours are present in high concentrations on the arc axis. It has been shown that diffusion driven by the electric field dominates in the helium arc, leading to diffusion directly upwards from the centre of the weld pool to the cathode [3, 4]. Comparison of the combined temperature and electric field diffusion coefficients for the Fe-Cr-He mixture with those for the Fe-Cr-Ar mixture, shown in Fig. 3, reveals that $\overline{D^E_{Fe}}$ and $\overline{D^E_{Cr}}$ are much larger for the helium case, so electric field diffusion is much stronger. Further, $\overline{D^T_{Fe}}$ and $\overline{D^T_{Cr}}$ are close to zero for the helium case for temperatures below 13 000 K, which Fig. 4(a) shows is the maximum temperature in the helium arc, so temperature diffusion has little influence.

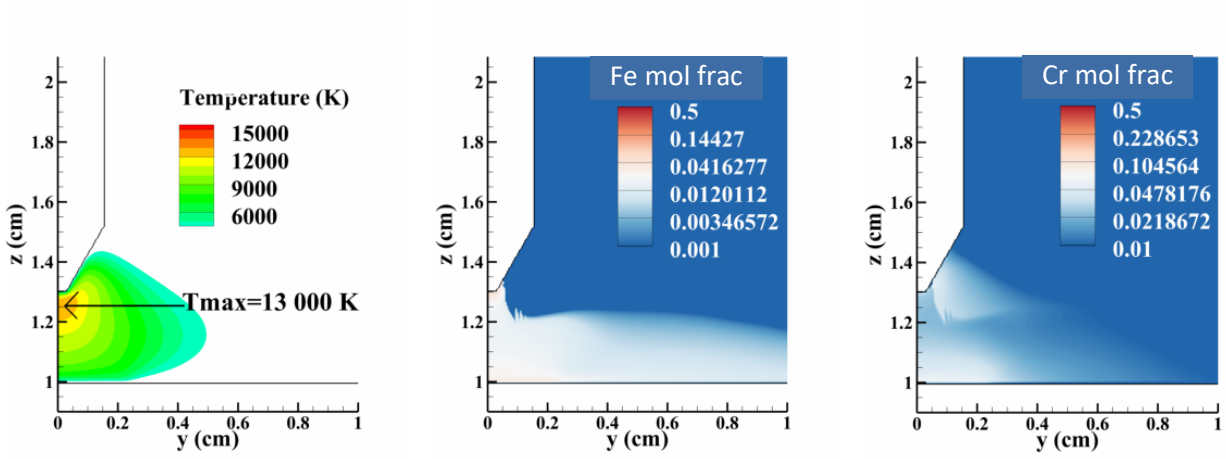

(a) (b) (c)

Fig. 4. Distributions of (a) temperature, (b) iron vapour mole fraction and (c) chromium vapour mole fraction in helium TIG welding of stainless steel.

5. Comparison with experiment

The results obtained for helium TIG welding have been shown by Park et al. [3, 4] to be in very good agreement with the emission spectroscopy measurements of Tanaka and Tsujimura [2]. In particular, the distributions of emission from Cr I and Fe I lines were found to agree with the predictions of the model. Moreover, measurements showing deposition of chromium, but not of iron, on the cathode at distances of ~2 mm above the tip were replicated by the model. This can be seen by comparing Figs 4(b) and (c), which show that the iron vapour is only present near the lower 0.05 mm of the cathode, while chromium vapour is present up to 2 mm above the cathode tip.

There are no corresponding measurements of metal vapour distribution in argon TIG welding. In fact, some studies (e.g. [5]) found no evidence of metal vapour in the arc column. However, a photograph of an argon arc with a stainless steel workpiece for the same conditions used in our model, reproduced in Fig. 5, shows the characteristic blue glow of metal vapour close to the cathode tip as well just above the workpiece. This is in accordance with our predictions for the regions of high concentrations of metal vapour, show in Fig. 1.

Fig. 5. Photograph of an argon TIG arc with a stainless steel workpiece, for the conditions used in the model. From [8]

6. Conclusions

A computational model of TIG welding with a stainless steel workpiece that takes into account the presence of metal vapour has been developed. Unlike previous models, two metal vapours can be treated simultaneously, and all important diffusion driving forces are taken into account.

In contrast to previous models, our model predicts that metal vapour is present near the cathode in both argon and helium arcs. This is attributed to diffusion driven by temperature gradients combined with the recirculating convective flow in the argon case, and diffusion driven by the electric field in the helium case. Experimental evidence for the presence of metal vapour near the cathode, consistent with the predictions of out model, has been presented in the literature.

7. References

[1] A. B. Murphy, Journal of Physics D: Applied Physics, **43**, 434001 (2010).

[2] M. Tanaka and Y. Tsujimura, Quarterly Journal of the Japan Welding Society, **30**, 164 (2012).

[3] H. Park, M. Trautmann, M. Tanaka, K. Tanaka and A. B. Murphy, Journal of Physics D: Applied Physics, **50**, 43LT03 (2017).

[4] H. Park, M. Trautmann, K. Tanaka, M. Tanaka and A. B. Murphy, Journal of Physics D: Applied Physics, **51**, 395202 (2018).

[5] A. J. D. Farmer, G. N. Haddad and L. E. Cram, Journal of Physics D: Applied Physics, **19**, 1723 (1986).

[6] M. Hertel, A. Spille-Kohoff, U. Füssel and M. Schnick, Journal of Physics D: Applied Physics, **46**, 224003 (2013).

[7] X. N. Zhang, A. B. Murphy, H. P. Li and W. D. Xia, Plasma Sources Science and Technology, **23**, 065044 (2014).

[8] M. Tanaka, K. Yamamoto, S. Tashiro, K. Nakata, E. Yamamoto, K. Yamazaki, K. Suzuki, A. B. Murphy and J. J. Lowke, Journal of Physics D: Applied Physics, **43**, 434009 (2010).